Available online at www.sciencedirect.com
ScienceDirect
Journal of the European Ceramic Society 26 (2006) 3153–3160
www.elsevier.com/locate/jeurceramsoc

Thick YSZ films prepared via a modified sol–gel route: Thickness control (8–80 μm)

M. Gaudon [a], Ch. Laberty-Robert [a,*], F. Ansart [a], P. Stevens [b]

[a] *CIRIMAT, LCMIE, UPS, Bat II R1, 118 route de Narbonne, 31062 Toulouse, Cedex 04, France*
[b] *EDF, European Institute for Energy Research, Karlsruhe, Germany*

Received 14 February 2005; received in revised form 30 August 2005; accepted 16 September 2005
Available online 19 October 2005

Abstract

Dip-coated suspensions were used for preparing YSZ layers on both dense and porous substrates. The microstructure of the as-obtained thick films was studied by varying the characteristics of the organic YSZ suspensions (concentration, viscosity, etc.) used as coating bath. The thickness and the microstructure of the films were found to depend on the YSZ powder content and on the polymeric sol/dispersant solution (EtOH–MEK) ratio of the suspensions. The porosity created in the films depends on the r_m ratio, e.g., the volume fraction of polymeric chains in the green layers. Finally, a comparison of the film thickness on dense and porous substrates showed that films prepared on porous substrates tend to exhibit higher thicknesses.

Accordingly, YSZ ceramic films with thickness varying in between 8 and 80 μm were prepared.

Keywords: Solid oxide fuel cell (SOFC); Suspensions; YSZ; ZrO_2; Sol–gel methods; Films

1. Introduction

A lower operating temperature (<700 °C) for solid oxide fuel cells (SOFCs) enables high temperature steels to be used as interconnect materials, which significantly decreases the cost of the cell, and increases the reliability of SOFC stacks.[1–6] However, the major drawback in decreasing the working temperature is that it greatly decreases the performance of the other cell components, especially the electrolyte.

Current SOFC development focuses on the research of new electrolyte materials exhibiting better ionic conductivity than the conventional yttria-stabilized zirconia (YSZ) at intermediate temperatures.[7] However, a thin film concept for electrode-supported designs based on the well-known YSZ is more promising, even though it has a lower ionic conductivity than other new materials. Keeping yttria-stabilized zirconia as electrolyte material, the electrolyte membrane should be as thin as possible in order to have ohmic losses in a cell at a tolerable level but thick enough to maintain gas tightness and avoid pin-holes. Among the other advantages of using thin electrolytes are the reduced materials costs and the improved fuel cell characteristics.[8] In anode supported SOFCs, good cell performances including timelife and power density were obtained with 10–20 μm YSZ electrolytes.[9–11]

So far, various thin film deposition methods have been used in the fabrication of electrolytes for intermediate temperature SOFC such as electrochemical vapor deposition (EVD),[12] physical vapor deposition (PVD),[13] vacuum plasma spraying,[14] tape-casting,[15] screen-printing,[16] and spray pyrolisis.[17] However, the sol–gel process method has seldom been applied for SOFC technology. The dip-coating of sol or gel is a coating technology that has the potential to produce thin (0.1–1 μm) and gas-tight (crack-free) ceramic layers on dense substrates.[18–22] However, it is difficult to prepare gas-tight film on a porous substrate, even by using multiple layer technology. In this work, a suspension made of sol and particles was investigated in order to increase the film thickness. To our knowledge, only few studies of the use of suspensions with the dip-coating technique have been presented to prepare films with a controlled thickness. Xia et al.[23] reported the use of YSZ powders in ethanol as dip-coated suspensions for the preparation of yttria-stabilized zirconia membranes on porous

* Corresponding author at: Naval Research Laboratory, Surface Chemistry Branch, Code 6171, 4555 Overlook Avenue, South West, Washington, DC 20375, USA. Tel.: +1 202 767 1344; fax: +1 202 767 3321.
E-mail address: laberty@ccs.nrl.navy.mil (Ch. Laberty-Robert).

0955-2219/$ – see front matter © 2005 Elsevier Ltd. All rights reserved.
doi:10.1016/j.jeurceramsoc.2005.09.026

substrates. Their YSZ powders were obtained via a soft chemistry route, namely coprecipitation. However, the films exhibit low thickness and cracks. A multilayer process was considered in order to prevent cracks and to obtain higher thickness. Some authors also mentioned the use of hybrid sol/powder systems to impregnate honeycomb.[24] The advantage of using a hybrid system is to limit the sol infiltration into the support pores while achieving satisfactory loading. These results are mostly correlated to the combination of the properties of the sols and the powders.

In this study, we develop a sol–gel-based strategy for the production of YSZ thick films with controlled thickness. Our approach to synthesize these films is based on the formulation of the dip-coated suspensions. These suspensions are obtained by mixing optimized slurries for tape casting and polymeric sol for dip-coating. A well-dispersed suspension of polymeric sol and ceramic particles was achieved by particles surface modification, which is very important in order to get homogeneous thick films. Upon mixing the two solutions (polymeric sol and YSZ dispersed in ethanol/methylethylcetone (60/40) (EtOH–MEK) azeotropic solution), a flocculation of particles with polymer occurs via electrostatic attraction and/or steric effect. Compared with common methods used to prepare thick films, our strategy has several advantages among which the fact that the formation of flocculated suspensions makes it possible to deposit the suspension via the dip-coating process on YSZ dense or porous substrates and to obtain homogeneous films. The morphology of the films, their porosity as well as their thickness, can be readily adjusted by changing the volume ratio of polymeric sol to EtOH–MEK solution and the powder content in the suspensions.

2. Experimental

2.1. Materials

Yttria-stabilized zirconia (8 mol% yttria cubic zirconia crystals) powders (TOSOH, Co) with an average particles size of 30 nm were used as materials in the experiments. The dispersant was commercial MELIORAN®, anionic surfactant (CECA France, Archema Group, viscosity: 30–35 mPa s). Two different substrates, with different microstructure and composition were used for the YSZ films synthesis. NiO–YSZ Cermets manufactured by InDEC,BV Company, Holland, were used as porous substrates. These substrates present pore sizes varying between 200 nm and 5 μm and an open porosity of ≈15%. YSZ ceramic pellets manufactured by LEPMI, INPG, Grenoble of 1 mm thick × 20 mm diameter were used as dense substrates. In order to get good adhesion on the YSZ ceramics, the substrates were first polished down to an average roughness of 10 nm.

2.2. Formulation of the suspensions and processing for YSZ films

YSZ thick films were prepared by dip-coating both porous or dense substrates in the suspension. The YSZ powder was first dispersed in EtOH–MEK (60–40) azeotropic mixtures by using a commercial dispersant (MELIORAN®). This dispersive solvent and dispersant were chosen according to Chartier's work on the formulation of slurries for tape-casting process.[25–27] In order to obtain a homogeneous suspension, 2.5% in weight of dispersant compared to YSZ powder was first dispersed in the azeotropic mixture and then powder (>20% in weight) was added under constant magnetic stirring. Attempts to synthesize suspensions using YSZ/MEK–EtOH solution had shown that no film was formed on the YSZ substrates using the dip-coating technique.[28]

A polymeric matrix may then be introduced to the suspension in order to obtain suitable wettability and viscosity (>5 mPa s), and then formation of uniform film. The polymeric solution was obtained from polycondensation reactions between hexamethylenetetramine (HMTA) and acetylacetone (Acac) in acetic acid. The molar ration between HMTA and Acac was 1:1. The viscosity of the polymeric matrix was adjusted by heating (∼70 °C, under constant stirring) and was kept constant to 30 mPa s. Preliminary investigations had shown that the state of dispersion of powders in this new mixture is affected by the order of introduction of the different additives.[28] Accordingly, this polymeric matrix was first added to the azeotrope media in which YSZ powders were first well dispersed by using Melioran as dispersant. The mixing of both solutions was then achieved by vigorous magnetic stirring during a couple of hours. Previous attempts had shown that in order to obtain films with a thickness superior to 1 μm, the powder content must be superior to 20% in weight. Lower powder content gave rise to film's thickness of 50–150 nm. This is mostly correlated to the low viscosity of the suspension for this powder loading (5 mPa s).

The rheological behavior of the dip-coated suspensions (YSZ powder/polymeric sol/MEK–EtOH solution) was then studied and it was shown to depend on the powder content and the volumetric ratio of polymeric sol/ azeotropic EtOH–MEK, so-called r_m. The number of polymeric chains in these dip-coated suspensions is correlated to the r_m ratio. In the flowchart of Fig. 1 are reported the key points of the synthesis process.

A withdrawal speed of 1.2 cm min^{-1} was used to prepare the films. After the dip-coating process, the YSZ films were dried at 100 °C and were then finally heated to the desired temperature (1300 °C) by using a ramp of 2 °C min^{-1}, kept at this temperature for 6 h and then allowed to cool to ambient temperature. Thermal treatments were performed in air. Preliminary experiments had shown that the drying rate of the as-prepared films affects the cracks number and morphology. The lower drying rate conduces to the formation of fewer cracks.[27] Accordingly, ambient temperature drying was first used for the as-prepared films.

2.3. Characterization

2.3.1. Rheology

A rheometer (Rheomat-115) was used to determine rheological properties of all suspensions at 25 °C. Each suspension was subjected to an increasing shear rate from 5 to 1000 s^{-1} with a speed varying in the range of 5 to 780 min^{-1}. The shear rate was then subsequently reduced to 5 s^{-1}.

Apparent viscosity of sols was measured with a rotating-spindle viscometer (Tve-05). The shear stress was 66.5 s^{-1}.

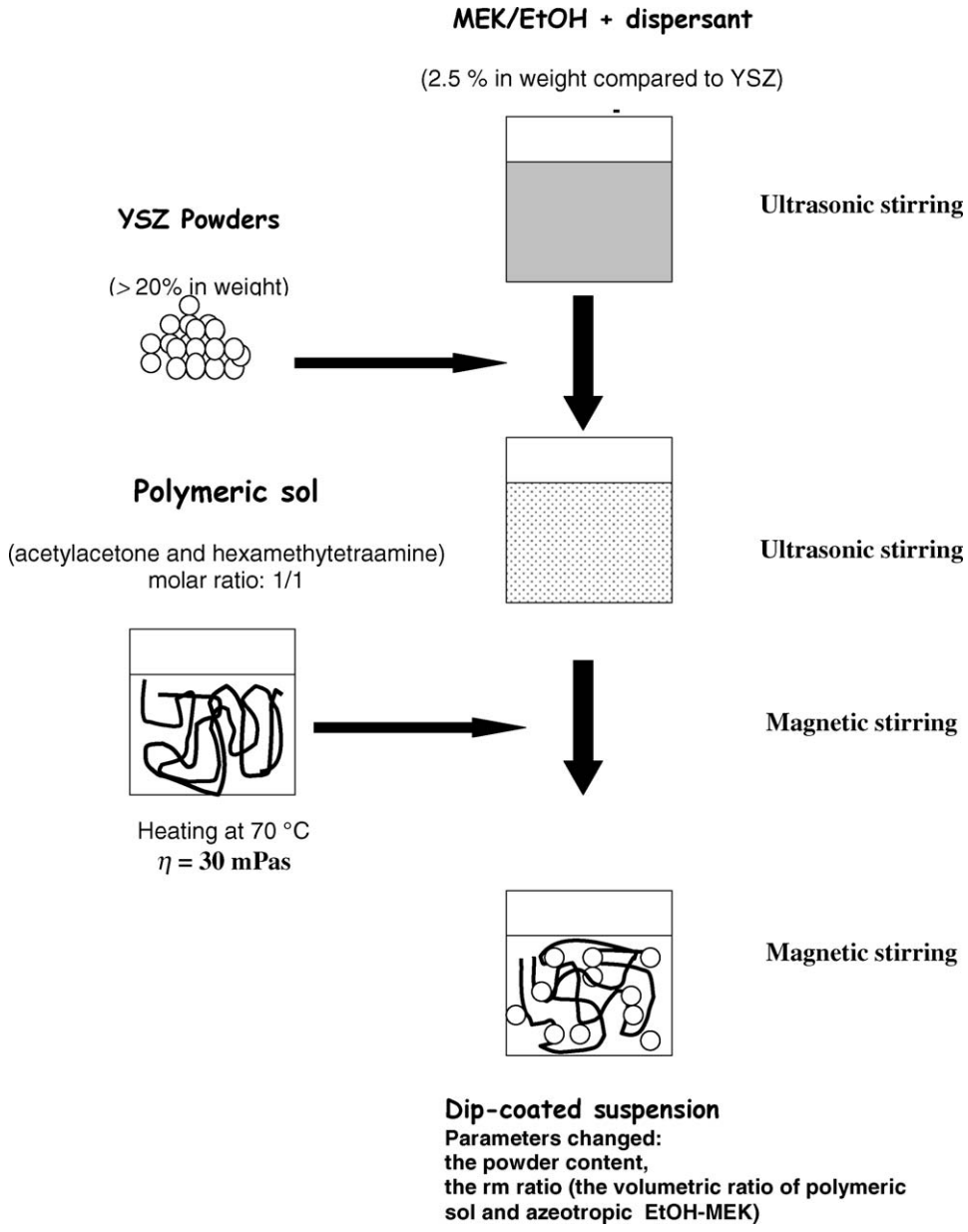

Fig. 1. Schematic of the YSZ dip-coated suspensions used in this work.

The apparent viscosity of sols was measured at this shear stress because it represents the conditions, which are reached at the interface suspension/substrate during the dip-coating process.

2.3.2. Sedimentation tests

Sedimentation tests were performed by pouring 50 mL of a given suspension into a 50 mL graduated Pyrex glass cylinder. Sediment heights were recorded after 72 h. In a typical suspension, 10 g of YSZ powder was first dispersed in EtOH–MEK solution and the polymeric sol was then added to it. The volumetric ratio between the polymeric sol and the EtOH–MEK solution (r_m) varied between 0.05 and 0.5.

2.3.3. Characterization of films

Thick films with different microstructures were prepared by using different powders content and r_m ratio.

XRD analysis was performed in order to confirm that the processing (heating, dip-coated process) has no influence on the crystallographic structure of the YSZ powders. Siemens D501 equipment was used for collecting X-rays diffraction data. The Cu Kα lines were used as a source.

Scanning electron microscopy (SEM) (JEOL-JSM6400) was used to investigate the morphology evolution of the as-deposited films after heat-treatment. The YSZ powder morphology was also determined from SEM analyses.

3. Results and discussion

3.1. Films on dense substrates

The microstructure of the films is highly dependent on the properties of the starting materials and the suspension prop-

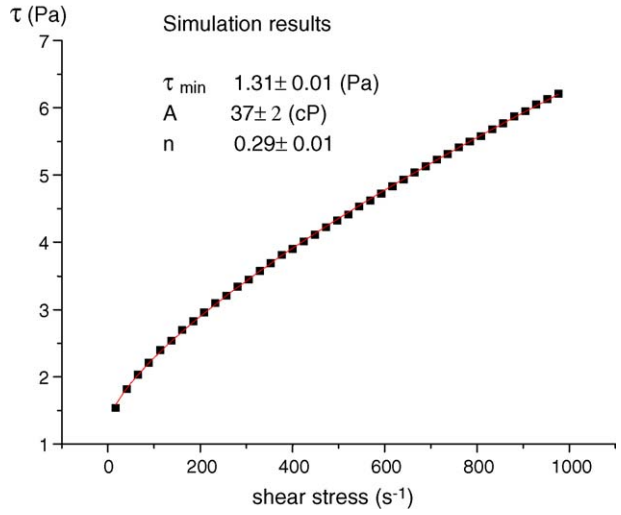

Fig. 2. Flow curves for organic YSZ suspension, 30 wt%.

erties, such as apparent viscosity, volume ratio of ceramic powders/polymeric sol and the volume ratio between the polymeric sol and the EtOH–MEK solution (r_m ratio). In order to get uniform films with this process, a key point is to prepare well-dispersed suspension of both particles and polymeric sol, otherwise pre-agglomeration of the powders produces films having cracks and high roughness.

3.1.1. Influence of the r_m ratio on the rheological behavior of the suspensions and the film microstructure

This study has been performed on concentrated YSZ suspensions (powder content of 30 wt.%) with different r_m ratios. Fig. 2 shows the flow curves at 25 °C (shear stress versus shear rate) of a typical suspension.

As shown, the suspension exhibits a viscoplastic behavior. The experimental data were adjusted to the described model using the following relationship: $\tau = A\gamma^{1-n} + \tau_{min}$, where A, n, and τ_{min} are constants, τ is the shear stress (Pa) and γ is the shear rate (s^{-1}) (Eq. (1)). A is expressed in Pa s^{-1} as viscosity, τ_{min} represents the threshold stress for liquid flow and n is characteristic of the difference between a newtonian and a viscoplastic rheological behavior. The viscoplastic behavior observed might be explained by the flocculation of particles in the suspensions, which is caused by nanoparticle-polymeric chains interactions. Indeed, the shear thinning flow behavior suggests that the flocculated particles in the suspensions were broken down into smaller flow units by the applied force during the rheological tests.

The corresponding rheological parameters of the model (A, n, and τ_{min}) obtained from suspensions of different r_m ratios are summarized in Table 1.

Table 1
n and τ_{min} values as function of the r_m ratio

r_m ratio	0	0.05	0.1	0.3	0.5
τ_{min}	0.51	2.64	1.79	0.98	0.82
A	4	7	17	31	30
n	0.12	0.08	0.18	0.23	0.25

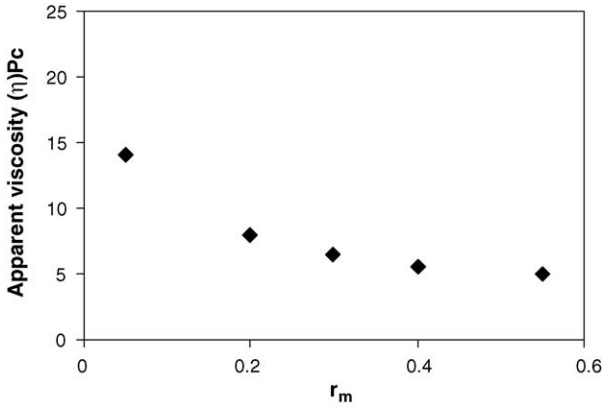

Fig. 3. Apparent viscosity variations as function of the r_m ratio at constant shear rate = 66.5 s^{-1}, for YSZ slurry, 30 wt.%.

As the r_m ratio increases, n increases while τ_{min} decreases. This indicates an increase of the floculated unit size. In parallel, the ability to break these flocculates increases, so that the resistance to flow was reduced, leading to a lower τ_{min}. In fact, polymeric chains and dispersed YSZ powders interact with each other to form a relatively flexible and coherent "network".

Measurements of the apparent slurry viscosity as a function of the r_m ratio at constant shear rates (66.5 s^{-1}) have shown a strong increase of the viscosity for low r_m ratio and an asymptotic viscosity variation in the range of r_m [0.05–0.5] (Fig. 3). Such a rheological behavior is comparable to the evolution of τ_{min} with r_m. This indicates that for low shear rates, the apparent viscosity is governed by the hardness of the polymeric/particles network.

The interaction between polymeric chains and particles is confirmed by sedimentation experiments on YSZ powders suspensions. The effect of the r_m ratio on the sedimentation height of the organic YSZ suspensions for time = 72 h is shown in Table 2. For $r_m = 0$ (suspensions without polymeric chains), a very high degree of dispersion is reached and no sediment was formed after 72 h. For polymeric suspensions, the results show that the sediment height or the settling time increases with the r_m ratio. This behavior indicates that some of the polymeric chains are present in the sediment and therefore that the polymeric chains are involved in the formation of the flocculates.

This rheological study has shown that our particulates flocculated and that flocculates correspond to a mixture between particles and polymeric chains. In our work, this specific situation, formation of a polymeric chains—solid particles "network", is suitable for making homogeneous films with a controlled thickness.

YSZ thick films are synthesized using suspensions with r_m varying from 0.5 to 0.05. The SEM micrographs of YSZ films for r_m ratio at 0.05 and 0.5, respectively is shown in Fig. 4. The

Table 2
Sedimentation height of organic YSZ suspensions as a function of the r_m ratio, time = 72 h

r_m ratio	0	0.05	0.2	0.5
Sediment height (mL)	No sediment	9.5	12	15

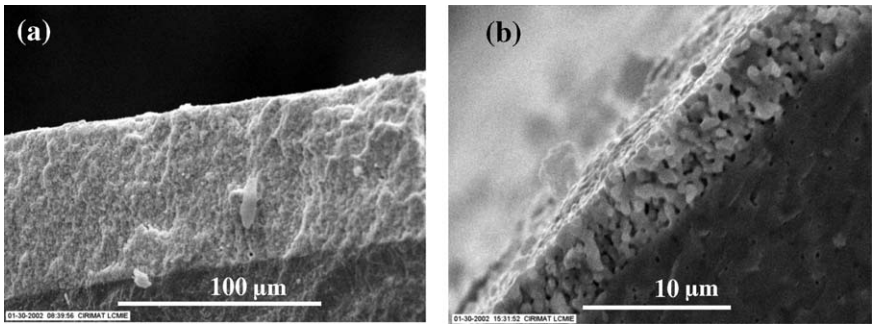

Fig. 4. Scanning electron micrographs of YSZ films heat-treated at 1000 °C in air for 2 h from slurries with $r_m = 0.05$ (a) and $r_m = 0.5$ (b).

films are continuous and homogeneous whatever the r_m ratio used in the suspensions. Fig. 4 shows that the films are porous whatever the r_m ratio. Their porosity is correlated to the presence of polymeric chains in the dip-coated suspensions. Nevertheless, the microstructure (film thickness and porosity) is sensitive to the r_m ratio. High r_m ratio in dip-coated suspensions corresponds to thinner green films with high volume fraction of polymeric chains. This is why thinner films still have porosity.

Note that for $r_m = 0$, no value is reported on the graph because of the inhomogeneity in the films that made the film thickness evaluation impossible. This particular point corresponds to a suspension without any polymer solution.

The evolution of the thickness as a function of the r_m ratio is described by a decreasing asymptotic function, shown in Fig. 5. One can see that the evolution of the layer thickness as a function of the r_m ratio presents similarities with the evolution of the apparent viscosity of the suspension (or shearing stress τ_{min}).

Thus, for an identical powder content in the suspensions, it is possible to reach films with different thicknesses and microstructure by changing the amount of polymeric chains in the suspensions.

3.1.2. Study of the powder content

The powder content in the suspensions is optimized in order to increase the film density. Note that changing the powder content in the YSZ suspension modifies, of course, the film thickness.

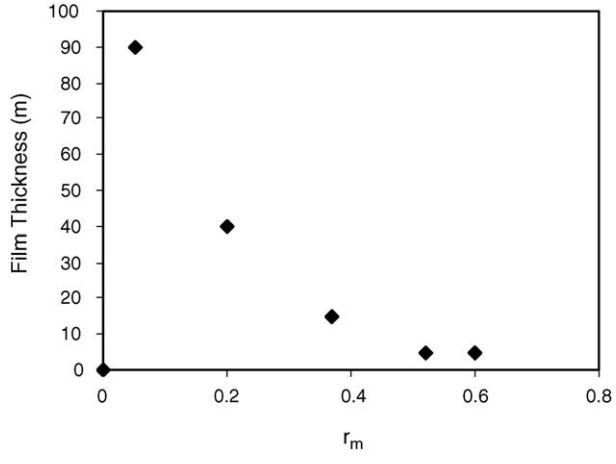

Fig. 5. Film thickness as a function of r_m ratio for 30 wt.% YSZ in the suspensions.

The SEM images of the cross-sectional view of YSZ films sintered at 1000 °C for 2 h for 60, 35, and 20 wt.% powder contents are shown in Fig. 6. The thickness of the films evolves with the powder content, and the cross-section microstructure remains the same whatever the thickness of the film. The film thickness was then determined from these data. Its evolution as a function of the powder content in the suspensions for $r_m = 0.25$ is reported in Fig. 7a. No linear variation of the film thickness with a coefficient of about 1.8 with a correlation factor R^2 of 0.9991 according to the following equation:

$$h = K_{exp} T\%^{1.8} \quad (1)$$

where h represents the film thickness, K_{exp} an experimental constant including the viscosity of the dip-coated solution, their density, the withdrawal speed and, $T\%$ the powder content in the dip-coated suspension. Note that the viscosity of the dip-coated solution had been previously studied. It had been shown that the films' thickness evolves as a function of the powder content inside the dip-coated solution. This behavior is comparable to the evolution of the films' thickness as a function of the powder content.

The increase in the film thickness with the powder content, ranging from 0 to 60%, is correlated to the apparent viscosity of the suspensions for a shear rate of 66.5 s^{-1}. In the studied range, the apparent viscosity of the suspension as a function of the powder content is reported in Fig. 7b, it follows a power function with a coefficient of 1.2:

$$\eta = K_1 T\%^{1.2} \quad (2)$$

with a correlation factor R^2 of 0.9996, where $T\%$ is the powder content, η the viscosity of the suspension and K_1 an experimental constant.

This increase in the apparent viscosity with the powder content can be related to two phenomena: the strong influence of the flocculated network or a stronger network due to an increase in the interactions between particulates and polymeric chains.

In the Landau and Levich law,[29] the authors showed that the film thickness (h_0) is a balance of three forces: the forces of gravity, the viscous drag force and the capillary force. In this case, the thickness of the film (h, µm) is proportional to the viscosity η (mPa s^{-1}), the surface tension (σ, mJ m^{-2}), the density of the coating bath (ρ, g cm^{-3}), the substrate speed withdrawal

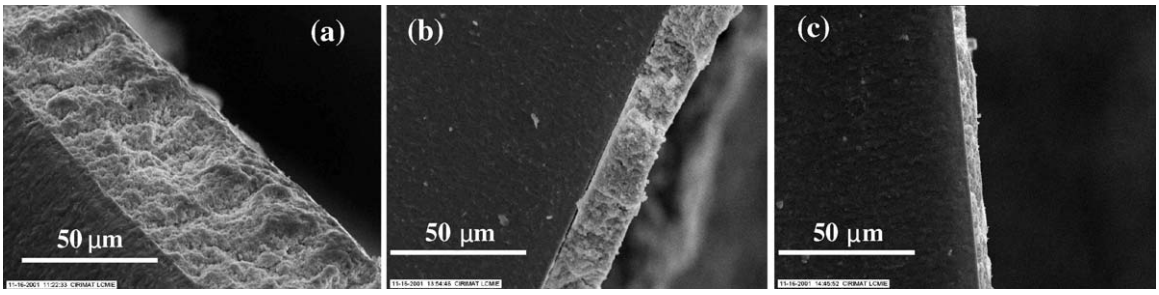

Fig. 6. Scanning electron micrographs of YSZ films heat-treated at 1300 °C in air for 2 h from dip-coated suspensions having different powder content: (a) 60 wt.%, (b) 35 wt.%, and (c) 20 wt.%.

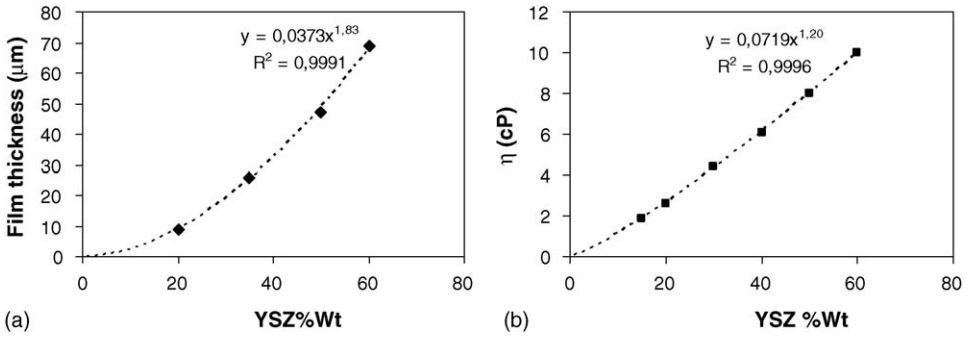

Fig. 7. Evolution of the film thickness (a) and apparent viscosity (b) as a function of the powder content in the dip-coated suspensions.

(U, cm min^{-1}), and the acceleration (g, N Pa) due to gravity:

$$h = K_2\left(\frac{\eta U}{\sigma}\right)^{1/6}\left(\frac{\eta U}{\rho g}\right)^{1/2} \quad (3)$$

Furthermore, considering that the density and the surface tension are independent on the powder content in the suspensions, in this study, the Landau and Levich law can be written as follows:

$$h = K_3 T\%\eta^{2/3} \quad (4)$$

By combining Eqs. (2) and (4), one can note that for these experiments, the Landau and Levich law seems to be respected[29] since the power function coefficient of Eq. (1) is confirmed. This result indicates that for a constant withdrawal speed, the viscosity of the suspension mostly governs the film thickness.

3.2. Coatings on porous substrates

Thick films of YSZ were also prepared on porous substrates, NiO–YSZ cermets. The cross-section of YSZ thick films synthesized from suspensions with 30% powder content and with various r_m is shown in Fig. 8. The films are homogeneous. However, comparisons between the film thickness on dense and porous substrates show that porous substrates generate higher thicknesses than their dense counterparts (Fig. 9). The films obtained for low r_m present a large number of cracks and, in some cases, a layers pilling phenomenon can be observed. In contrast, the films obtained for high r_m are homogeneous and do not present cracks. In order to understand the formation of cracks, we have checked the morphology of films calcined at various temperatures (not shown here). Those experiments have shown that cracks appear at high temperature, 600 °C and are correlated to the films' thickness. The thinner the films, the lower the number of cracks. This result suggests that cracks in the

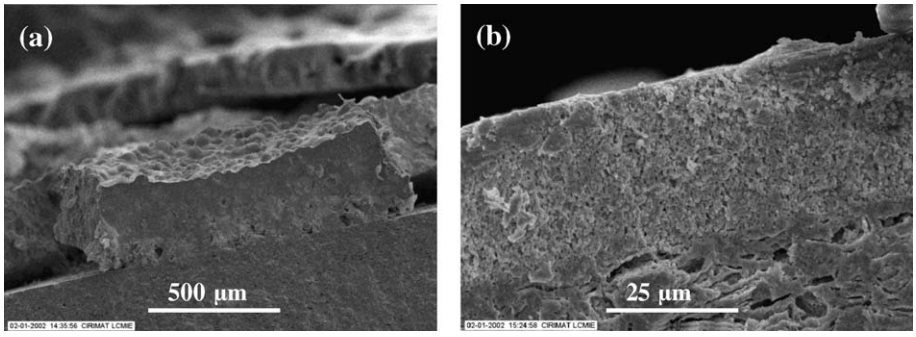

Fig. 8. SEM micrographs of films on porous substrates: (a) $r_m = 0.08$ and (b) $r_m = 0.5$.

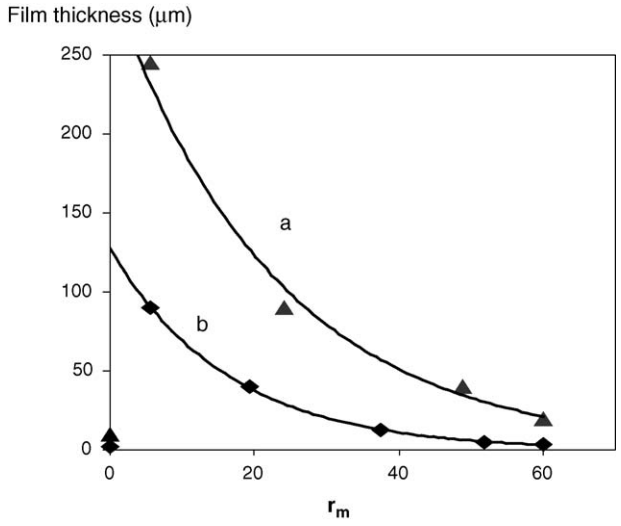

Fig. 9. Evolution of the film thickness as function of the r_m ratio for: (a) porous and (b) dense substrates. Powder content in the suspension of 50 wt.%.

films are mostly due to the decomposition of organics in the as-prepared films for porous substrates. Indeed, the higher the deposited film thickness, the higher the organic content in the films (even if the volume fraction of polymeric chains in the green films decrease with the thickness). That is why cracks cannot be suppressed during the heat-treatment step because of the high-level of the organic content.

The influence of the powder content in the suspensions, on the film thickness has been studied. As was the case for dense substrates, their thickness increases with the powder content in the suspensions. Nevertheless, this evolution is more rapid for porous substrates and cannot be described by the Landau and Levich law. An additional capillarity effect caused by the infiltration of a part of the suspension into the substrates pores may explain why thicker films are formed on porous substrate and why the Landau and Levich law is not respected.

The processing technique used in this work enables us to synthesize homogeneous films with a controlled thickness. The thickness can vary in the range of 8–80 μm. Nevertheless, films are still porous even after changing r_m and powder content in the dip-coated suspensions. However, this characteristic has to be optimized in order to be able to use this process in the manufacturing of gas-tight electrolytes for SOFC devices.

4. Conclusion

Thick porous YSZ films were deposited on dense and porous substrates by the dip-coating technology. This technique was chosen because it is a simple and low cost technology to coat planar or three-dimensional surface, which can be further used for industrial applications. A suspension composed of solvent, powder and polymeric sols was dip-coated on both porous and dense substrates. The thickness of the coating was adjusted by the powder content in the suspensions and the fraction of polymeric chains added (r_m ratio). The as-synthesized films were homogeneous and crack-free after heat treatment at 1300 °C in air. However, whatever the r_m ratio, the sintered films have pores. The thickness obtained so far varies between 8 and 80 μm. The major parameters affecting the film's microstructure are the powder content and the r_m ratio.

Acknowledgements

This work results from a joint program funded by EDF and ADEME. The authors would like to thank Nathalie Thibaud (ADEME) for her support.

References

1. Steele, B. C. H., *Solid State Ionics*, 2000, **134**(1/2), 3–20.
2. Minh, T. N. Q. and Takahashi, T., *Science and Technology of Ceramic Fuel Cells*. Elsevier, Amsterdam, 1995, pp. 165–198 and 233–306.
3. Brylewski, T., Namko, M., Maruyama, T. and Prybylski, K., *Solid State Ionics*, 2001, **143**(2), 131–150.
4. Huang, K. Q., Hou, P. Y. and Goodenough, J. B., *Solid State Ionics*, 2000, **129**(1–4), 237–250.
5. Stambouli, A. B. and Traversa, E., *Renewable Sustainable Energy Rev.*, 2002, **6**, 433.
6. Winkler, W. and Koeppen, J., *J. Power Sources*, 1996, **61**(1/2), 201–204.
7. Minh, N. Q., *Proceedings of the 4th International Symposium on Solid Oxide Fuel Cells*, eds. M. Dokiya, M. Yamamoto, H. Tagawa and S. C. Singhal. 1995, pp. 138–145.
8. Barnett, S., *Energy*, 1990, **15**(1), 1–9.
9. Simwonis, D., Thülens, H., Dias, F. J., Naoumidis, A. and Stöver, D., *J. Mater. Process. Technol.*, 1999, **92/93**, 107–111.
10. Charpentier, P., Fragnaud, P., Schleich, D. M. and Gehain, E., *Solid State Ionics*, 2000, **135**(1–4), 373–380.
11. Fuel cell energy, In *Seca Annual Meeting*, Inc and Versa Power Systems, Pacific Grove, CA. 2005.
12. Carolan, M. F. and Michaels, J. N., *Solid State Ionics*, 1990, **37**(2/3), 189–196.
13. Honegger, K., Batawi, E., Spercher, C. and Diethelm, R., *Proceedings of the 5th International Symposium on Solid Oxide Fuel Cells*, *vol. 97-18*, ed. U. Stimming, S. C. Singhal, H. Tagawa and W. Lehnert. Electrochemical Society, Pennington, NJ, 1997, pp. 321–329.
14. Lang, M., Henne, R., Shaper, S. and Schiller, G., *J. Therm. Spray Technol.*, 1997, **10**(4), 618.
15. Minh, N. Q. and Montgomery, K., *Proceedings of the 5th International Symposium on Solid Oxide Fuel Cells*, *vol. 97-18*, ed. U. Stimming, S. C. Singhal, H. Tagawa and W. Lehnert. Electrochemical Society, Pennington, NJ, 1997, pp. 153–159.
16. Van Herle, J., Ihringer, R., Cavieres, R. V., Constantin, L. and Bucheli, O., *J. Eur. Ceram. Soc.*, 2001, **21**(10/11), 1855–1860.
17. Perednis, D. and Gauckler, L. J., *Solid State Ionics*, 2004, **166**(3/4), 229–240.
18. Chen, C. C., Nasrallah, M. M. and Anderson, H. U., *Solid State Ionics*, 1994, **70/71**, 101–108.
19. Gaudon, M., Laberty-Robert, Ch., Ansart, F., Stevens, P. and Rousset, A., *J. New Mater. Electrochem. Syst.*, 2002, **5**(1), 57–61.
20. Fontaine, M. L., Laberty-Robert, Ch., Ansart, F. and Tailhades, P., *J. Solid State Chem.*, 2004, **177**(4/5), 1471–1478.
21. Okubo, T., Takahashi, T., Sadakata, M. and Nagamoto, H., *J. Membr. Sci.*, 1996, **118**, 151–157.
22. Okubo, T., Takahashi, T., Nair, B. N., Sadakata, M. and Nagamoto, H., *J. Membr. Sci.*, 1997, **125**, 311–317.
23. Xia, C., Zha, S., Yang, W., Peng, R., Peng, D. and Meng, G., *Solid State Ionics*, 2000, **133**(3/4), 287–294.

24. Agrafiotis, G., Tsetsekou, A., Stournavas, C. J., Julbe, A., Dalmazio, L. and Guizard, C., *J. Eur. Ceram. Soc.*, 2002, **22**(1), 15–26.
25. Raeder, H., Simon, C., Chartier, T. and Toftegaard, H. L., *J. Eur. Ceram. Soc.*, 1994, **13**(6), 485–492.
26. Chartier, T., Hinczewski, C. and Corbel, S., *J. Eur. Ceram. Soc.*, 1999, **19**(1), 67–74.
27. Chartier, T., Merle, D. and Besson, J. L., *J. Eur. Ceram. Soc.*, 1995, **15**(2), 101–108.
28. Gaudon, M., Thesis University of Toulouse, 2001, pp. 163–165.
29. Landau, L. D. and Levich, V. G., *Acta Phys. Chim. USSR*, 1942, **17**, 42–54.